CHALMERS
UNIVERSITY OF TECHNOLOGY

A spherical probability distribution model of the user-induced mobile phone orientation

Citation for the original published paper (version of record):
Glazunov, A., Lehne, P. (2018). A spherical probability distribution model of the user-induced mobile phone orientation. IEEE Access, 6: 37185-37194.
http://dx.doi.org/10.1109/ACCESS.2018.2839960

IEEE Access
Multidisciplinary ⋮ Rapid Review ⋮ Open Access Journal

Received April 22, 2018, accepted May 17, 2018, date of publication May 23, 2018, date of current version July 25, 2018.

Digital Object Identifier 10.1109/ACCESS.2018.2839960

A Spherical Probability Distribution Model of the User-Induced Mobile Phone Orientation

ANDRÉS ALAYÓN GLAZUNOV[1,2], (Senior Member, IEEE), AND PER HJALMAR LEHNE[3]

[1]Department of Electrical Engineering, University of Twente, 7500 Enschede, The Netherlands
[2]Department of Electrical Engineering, Chalmers University of Technology, 412 58 Gothenburg, Sweden
[3]Telenor Research, 1331 Fornebu, Norway

Corresponding author: Andrés Alayón Glazunov (a.alayonglazunov@utwente.nl)

This work was supported in part by a project within the VINNOVA funded Chalmers Antenna Systems VINN Excellence Centre, Chalmers, and in part by Telenor.

ABSTRACT This paper presents a statistical modeling approach of the real-life user-induced randomness due to mobile phone orientations for different phone usage types. As well-known, the radiated performance of a wireless device depends on its orientation and position relative to the user. Therefore, realistic handset usage models will lead to more accurate over-the-air characterization measurements for antennas and wireless devices in general. We introduce a phone usage classification based on the network access modes, e.g., voice (circuit switched) or non-voice (packet switched) services, and the use of accessories, such as wired or Bluetooth handsets, or a speaker-phone during the network access session. The random phone orientation is then modeled by the spherical von Mises-Fisher distribution for each of the identified phone usage types. A finite mixture model based on the individual probability distribution functions and heuristic weights is also presented. The models are based on data collected from built-in accelerometer measurements. Our approach offers a straightforward modeling of the user-induced random orientation for different phone usage types. The models can be used in the design of better handsets and antenna systems as well as for the design and optimization of wireless networks.

INDEX TERMS Antennas and propagation, channel models, statistical distribution, over-the-air testing, phone usage model, von Mises–Fisher distribution.

I. INTRODUCTION

User-induced randomness of the phone orientation has been known to influence the performance of wireless devices, such as mobile phones. User-induced randomness is understood here as the variation of the usage positions of wireless devices in real-life situations. Currently, fixed usage type positions are largely based on the hypothesis that certain phone orientations should dominate depending on the services accessed. However, they do not fully describe the actual span of possible usage positions of a mobile phone. These are needed for devising realistic Over-The-Air (OTA) performance testing of wireless devices capable of providing satisfactory Quality-of-Service (QoS) to end users [1].

The device performance is sensitive to the propagation environment which in turn depends, among other things, on the usage mode of the device, e.g., device orientation in voice or non-voice modes [2], [3]. In OTA testing, two edge environments can be defined: the RIMP (Rich Isotropic MultiPath) environment and the Random-LOS (Random Line-OF-Sight) environment. In RIMP, the transmit signal reaches the receive antenna isotropically through various propagation paths. On the other hand, in Random-LOS there is only one path, i.e., the direct signal path between the transmit and receive antennas that is subjected to user-induced randomness. In RIMP, performance is independent from the device orientation; yet, it depends on the device usage, e.g, power absorption, impedance mismatch/detuning or both, as a result of the user body and different usage positions. In Random-LOS, randomness is induced mainly by the usage position and orientation relative the base station. This results in a random Angle-of-Arrival (AoA) and polarization of the incoming waves. Hence, the characterizations of wireless devices can be readily done in terms of polarization deficiencies of antennas and their impact on throughput performance as shown in [4] and [5]. The OTA performance in RIMP can be tested in reverberation chambers. On the other hand, OTA performance in ''pure-LOS'' has been traditionally characterized in anechoic chambers. Hence, performance in Random-LOS can be measured in anechoic chambers too.

It has already been demonstrated that random device orientation affects the propagation characteristics [6]. In the recently introduced Random-LOS OTA characterization

method, which uses the eponymous channel model, the effect of user-induced randomness on the system performance is naturally integrated [7]–[9]. Initial work pertaining the characterization of the user-induced randomness has been presented in [10] and [11]. However, currently available OTA tests do not take into account the user-induced randomness, but only fixed usage types, due to non-existing probabilistic usage models of modern versatile (smart) mobile phones.

In order to fill the aforementioned knowledge gap we present here the first systematic model addressing the user-induced mobile phone orientation randomness for voice and non-voice applications. The relevance of making such a model follows from the fact, among other things, that there is a need to produce OTA tests of antennas and wireless devices that incorporate actual user orientation in a realistic and relevant manner. The scope of this paper is therefore to use collected accelerometer sensor data from smart phones and analyze them in order to suggest a proper model for the device orientation [11]. The underlying method of collecting data from smart phones for this purpose, can also be adapted for use in, e.g., network optimization to improve use experience based on knowledge about usage modes, however this is outside the scope of the current work. Moreover, it is worthwhile to note that directly monitoring the usage type is not possible without doing changes in the network, which is also outside the scope of the presented work.

The contributions of this paper are summarized as follows:

- We suggest an approach to extract relevant data from accelerometer measurements obtained with Android phones by combining outlier removal with duplicate data removal.
- We introduce a usage type classification that follows a user's access to network services in terms of the two possible modes: voice (meaning circuit switched) or non-voice (meaning packet switched) and with the corresponding use of speaker and wired- or Bluetooth-headset following the user's natural behaviour. Hence, no pre-defined usage type positions are investigated, but the focus is on a user's real-life handling of the phones.
- We propose the von Mises-Fisher (vMF) distribution, i.e., the equivalent of the Gaussian distribution defined on the unit sphere [12] to model the statistical probability distribution function of the orientation of mobile phones for each specific usage type.
- An easy-to-use finite mixture model (FMM) is presented based on individual vMF distributions and on heuristic mixing probabilities corresponding to different phone usage types. The provided vMF distributions as well as the vMF FMM can be used to reproduce the desired random realizations of the user-induced orientations of the mobile phones and used as an input to further analysis, e.g., OTA characterization of mobile phones, or wireless network simulations.
- The extracted model parameters corresponding to the phone usage types classification are mapped to the classification of a phone's orientation in spherical coordinates given in [11]. Then, in order to harmonize our study with the existing fixed usage type definitions, e.g., defined by 3GPP we infer corresponding usage types from the analyzed accelerometer data. In this way, the provided model becomes more useful for the objective of standardized OTA methods.

The remainder of the paper is organized as follows: In Section II we present a description of the data collection and classification corresponding to different usage of a mobile phone for voice and non-voice service types, here we also present a straightforward method to select data representative of user-induced randomness. In Section III we introduce the von Mises-Fisher directional distribution model of the device orientation and validation procedure based on Quantile-Quantile plots (Q-Q plots). Section IV presents an analysis of the modelling results. Also here we suggest a finite mixture model for the identified phone usage types. A mapping of phone usage types to typical usage positions, assumed by 3GPP, is provided too. Conclusions and future work are outlined in Section V.

II. ACCELERATION DATA COLLECTION AND INTERPRETATION

A. MEASUREMENTS AND DATA CLASSIFICATION

Modern smart phones offer ample opportunities in their sensor capabilities. In this paper we use the built-in 3D linear acceleration sensors (i.e., the accelerometer) to determine the device orientation. The acceleration vector components are given in the device local coordinate system and delivers values in m/s^2. The measured values include the gravity acceleration vector. If the phone is stationary the length of the vector is $g = 9.8\text{m/s}^2$ (or other more exact value that depends on the actual geographical location). The device local coordinate system definition for Android phones is shown in Fig. 1 [13], where the positive direction is defined as the direction of increased acceleration. This means that the gravity acceleration vector is pointing away from the Earth's centre.

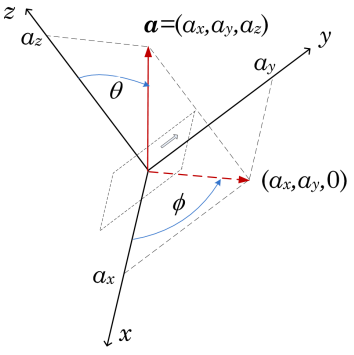

FIGURE 1. Gravity acceleration vector in the device coordinate system.

A smart phone application (app) has been installed onto a number of phones, and the data has been uploaded to a server which aggregates the data automatically into a searchable

database [10]. This app records sensor values from the phone in the background while the smart phone is active, i.e., during a phone call or non-voice session. The app collects samples approximately once per second. The phones belonged to ordinary users, and no instruction of specific behaviour was given, since we wanted to record the normal usage. Once installed and registered, the app was running as a background service on the phone, and was not interacting in any way with the user. Hence, during a service session the user behaves naturally, i.e., carries out with her common behaviour while using the mobile phone.

TABLE 1. Binary category classification of accelerometer data used to define phone usage type.

Bit	0	1
Service	VOICE	NON-VOICE
Wired-Headset	NO	YES
Speaker-Phone	OFF	ON
Bluetooth-Headset	OFF	ON

The data is further classified into four binary and self-explanatory categories as shown in Table. 1. The voice service in this context means circuit switched (CS) voice, not VoIP services like Skype or Viber which belong to the non-voice services. The value 0 is prescribed to the voice service, and to the NO and OFF specifications, while at the same time prescribing the value 1 to the non-voice service, and to the YES and ON specifications we get a 4−bit binary representation of the data giving 16 possibilities in total, out of which only some make practical sense. For example, a user that during voice service doesn't use a wired-headset, a speaker phone or a Bluetooth-headset can be denoted as *phone usage type:* 0000. Another user, that during non-voice service, uses a wired-headset, a speaker phone and a Bluetooth-headset can be denoted as *phone usage type:* 1111. The likelihood of observing phone usage type 0000 is high since it corresponds to the traditional way to talk over the phone. On the other hand phone usage type 1111 doesn't really make sense in a practical scenario.

B. ACCELERATION DATA MODELLING AND ESTIMATES

The gravity acceleration vector is used to estimate the accelerometer orientation [14]. The collected acceleration data is modelled by two terms

$$\boldsymbol{a} = \boldsymbol{R}\boldsymbol{g} + \boldsymbol{a}_{\mathrm{e}}, \tag{1}$$

where each data sample i is actually a 3D vector $\boldsymbol{a}_i = (a_{xi}, a_{yi}, a_{zi})$, $\boldsymbol{g}$ has the same magnitude as the gravity acceleration vector, but is directed in the opposite direction, i.e., upwards. If there are no other forces than gravity acting upon the device, i.e., the device is still or moving at a uniform rectilinear velocity, then $\boldsymbol{a}_{\mathrm{e}} = 0$. In this case, the measured acceleration is just the projection of the vector $\boldsymbol{g}$ into the local coordinate system of the device. Hence, the change of direction of the vector $\boldsymbol{g}$ is determined by the rotation matrix $\boldsymbol{R}$, such that $\|\boldsymbol{R}\boldsymbol{g}\| = g$, where the symbol $\|\boldsymbol{x}\|$ denotes the Euclidean norm of vector $\boldsymbol{x}$. Additive errors are modelled by $\boldsymbol{a}_{\mathrm{e}}$ since the actual non-inertial movement pattern (due to acceleration or deceleration) of the user is not known. The true distribution of $\boldsymbol{a}_{\mathrm{e}}$ is not known either nor are the distributions of the elements of the rotation matrix $\boldsymbol{R}$.

The above physical arguments lead us to the following observations: first, the acceleration data samples can be considered *random*; secondly, there may be *outliers* (i.e., samples that are much larger or smaller than the rest of the samples), and thirdly, ambiguity in acceleration data samples can be reduced by choosing those which magnitude is close to the magnitude of the *gravity acceleration vector*, i.e., $\|\boldsymbol{a}\| \approx g$. Following these observations we seek to remove outliers from data samples that are much larger or much smaller than g. To identify and remove outliers from the data we use the $1.5IQR$-*rule*. A data sample $\boldsymbol{a}_i$ is considered an outlier if $\|\boldsymbol{a}_i\| > Q_3 + 1.5IQR$ or $\|\boldsymbol{a}_i\| < Q_1 - 1.5IQR$, where $IQR = Q_3 - Q_1$ is the Inter-Quartile Range, Q_1 and Q_3 are the 25%− and the 75%−quartiles, respectively. We use the fact that the size of the IQR is an indication of the spread of the middle half of the data. In our case it should be concentrated in a very narrow region around Q_2, the 50%−quartile, i.e., the median.

Removing the outliers will have a filtering effect on the measurement data, which is a desirable effect since it improves the quality of the data. Other errors, e.g., due to hardware impairments, noise etc., are not considered here. Their importance will become apparent only for very accurate estimations of the user location [15], [16].

Another aspect related to the data quality or the number of useful samples, i.e., measurements coming from completely random user positions. For example, in realistic situations, it is unlikely to observe a large number of identical consecutive acceleration values. This is because, the movement pattern of a user is not completely stationary. Stationarity of users is outside the analysis presented here. However, we suggest, as a first step toward reducing measurement artifacts to take into account only *unique acceleration samples*. In this way, we remove duplicate data that cannot be clearly understood or that is not representative for the general usage patterns of mobile phones. In the future, as the size of data base increases, especially with measurements coming from a large number of different users, more sophisticated data processing will become necessary.

Hence, in this paper we remove data artifacts following two criteria: a data sample must not be an outlier, i.e., the acceleration vector can't be much larger or smaller than g and it's components must be unique. Next we present a statistical distribution model for user-induced mobile phone orientation.

III. SPHERICAL MODEL OF THE DEVICE ORIENTATION AND VALIDATION PROCEDURE

The actual orientation of a device is given by the θ and ϕ angles as shown in Fig. 1. We propose here an equivalent way that we believe is more meaningful and useful.

TABLE 2. Estimated parameters corresponding to the von Mises-Fisher directional probability distribution function, i.e., the concentration parameter $\hat{\kappa}$, and the mean direction vector $\hat{\mu}$ in Cartesian co-ordinates and the corresponding orientation angles in spherical coordinates, $\hat{\phi}_\mu$ and $\hat{\theta}_\mu$. Heuristic finite mixture model (FMM) weights π_{ijkl} and the number of samples $N_{s,ijkl}$ used to compute them.

Ph. Usage	vMF Distribution Parameters						FMM	
$\{ijkl\}$	$\hat{\kappa}$	$\hat{\mu}_x$	$\hat{\mu}_y$	$\hat{\mu}_z$	$\hat{\phi}_\mu$, [°]	$\hat{\theta}_\mu$, [°]	π_{ijkl}	$N_{s,ijkl}$
0000	3.23	0.27	0.93	0.24	73.97	76.37	0.5433	47988
0001	1.88	0.87	0.50	−0.01	29.88	90.75	0.0494	4365
0010	4.17	0.23	0.82	0.52	74.01	58.51	0.0262	2312
0100	2.10	0.08	0.30	0.95	75.69	17.85	0.2253	19903
1000	1.37	−0.04	0.65	0.76	93.73	40.85	0.0694	6134
1010	4.99	−0.06	0.88	0.47	93.78	62.01	0.0365	3221
1100	3.39	0.08	0.80	0.59	84.44	53.73	0.0499	4405

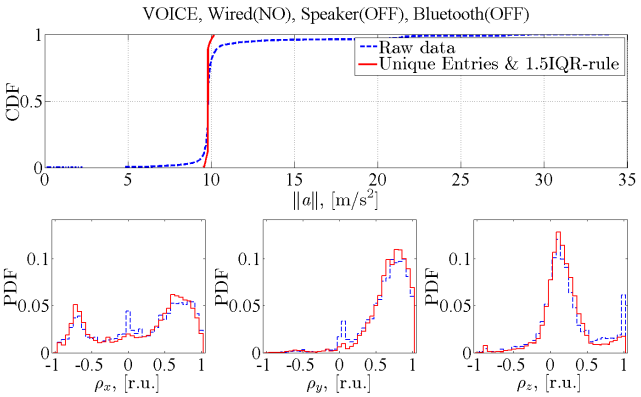

FIGURE 2. Example of empirical Cumulative Distribution Function of the magnitude of the measured acceleration $\|a\|$ (upper subplot) and the corresponding empirical Probability Distribution Function of the three cartesian components of the orientation vector ρ. Plots corresponding to the raw data and to data after removing outliers are shown for voice service users that used no wired-headset, no speaker-phone and no Bluetooth-headset, i.e. usage type: 0000.

A. THE VON MISES-FISHER (vMF) DIRECTIONAL DISTRIBUTION

Indeed, from the physical considerations stated above we can see that the actual orientation of the device is given by the orientation of the gravity acceleration vector in the device local coordinate system *xyz*. In this case the tip of the "random" vector $\boldsymbol{g}$ defined in this *xyz*-system will lay on the sphere with radius g. Hence, it is enough to define the vector indicating the orientation of the mobile phone device, i.e., an *orientation vector*. For acceleration data sample i we define it as

$$\boldsymbol{\rho}_i = \frac{\boldsymbol{a}_i}{\|\boldsymbol{a}_i\|}, \tag{2}$$

where $\boldsymbol{\rho}_i = (\rho_{ix}, \rho_{iy}, \rho_{iz})$ with $\|\boldsymbol{\rho}_i\| = 1$.

A useful model describing the statistical distribution of a unit vector $\boldsymbol{\rho} \in \mathbb{R}^3$ is the von Mises-Fisher (vMF) probability distribution function (pdf) [12]

$$f(\boldsymbol{\rho}; \boldsymbol{\mu}, \kappa) = \frac{\kappa}{4\pi \sinh(\kappa)} \exp(\kappa \boldsymbol{\mu}^{\mathrm{T}} \boldsymbol{\rho}), \tag{3}$$

where the parameter $\boldsymbol{\mu}$ with $\|\boldsymbol{\mu}\| = 1$, is the *mean direction* and $\kappa > 0$, is the *concentration parameter*. The distribution is rotationally symmetric around the mean direction $\boldsymbol{\mu}$, which provides the direction of concentration of data. The higher the spread of the data, the lower is κ, and viceversa. For uniformly distributed points on the sphere (i.e., isotropically distributed), $\kappa = 0$ and (3) becomes $f(\boldsymbol{\rho}) = \frac{1}{4\pi}$; no mean direction can be defined in this case. The maximum-likelihood estimators of the two parameters $\hat{\boldsymbol{\mu}}$ and $\hat{\kappa}$ are known and are computed following the results provided in [17]. For the sake of completeness of exposition the estimators are given in Appendix.

There are known algorithms to generate random vectors $\boldsymbol{\rho}$ following the distribution (3) [18]. In our computations we use the MATLAB® script provided in [19].

B. Q-Q PLOTS FOR THE vMF DIRECTIONAL DISTRIBUTION

The vMF distribution parameters, $\hat{\boldsymbol{\mu}}$ and $\hat{\kappa}$, i.e., the estimates of the mean direction and the concentration parameter, respectively, fully define our model of the directional data. However, we need to assess how well the model fits our data. An illustrative way is just plotting the normalized acceleration vectors or orientation vectors (2). However, given the large number of measurement points this is not a very practical way. Besides, we need a more meaningful approach. In this paper we use the so-called Quantile-Quantile plot or Q-Q plot for short. A Q-Q plot is a graphical method showing the quantiles of one probability distribution against the quantiles of another probability distribution. Hence, two probability distributions can be definitely compared and if two data samples come from the same probability distribution or data comes from the same theoretical probability distribution as the model then the Q-Q plot is a straight line. It is worthwhile to note that the Q-Q plot only gives an approximate idea of the underlying distribution.

In our analysis we use the Q-Q plot concept for directional statistics introduced in [20]. It is straightforward to implement, to interpret and it has many other advantages therein. The applicability of the method, i.e., the new quantile definition is restricted to the class of directional probability distributions with bounded density, admit a unique median direction, and are rotationally symmetric about the mean direction, which are satisfied by the vMF distribution. Due to practical reasons, we consider in this paper the empirical version for computing the *projection quantile*, i.e., $\hat{c}_\tau$. For a given quantile $\tau \in [0, 1]$, the corresponding projection $\tau-$quantile is obtained in three steps: (1) estimate the median $\boldsymbol{\mu}$ by an estimator $\hat{\boldsymbol{\mu}}$, (2) project all observations onto $\hat{\boldsymbol{\mu}}$, i.e., the projected population is $\boldsymbol{\rho}^{\mathrm{T}} \hat{\boldsymbol{\mu}}$ and (3) use a traditional definition of univariate quantiles for determining the $\hat{c}_\tau$.

IV. DATA PROCESSING, MODEL FITTING RESULTS AND ANALYSIS

The analysis includes data that has been collected from 11 users which used 7 different smart phone models from

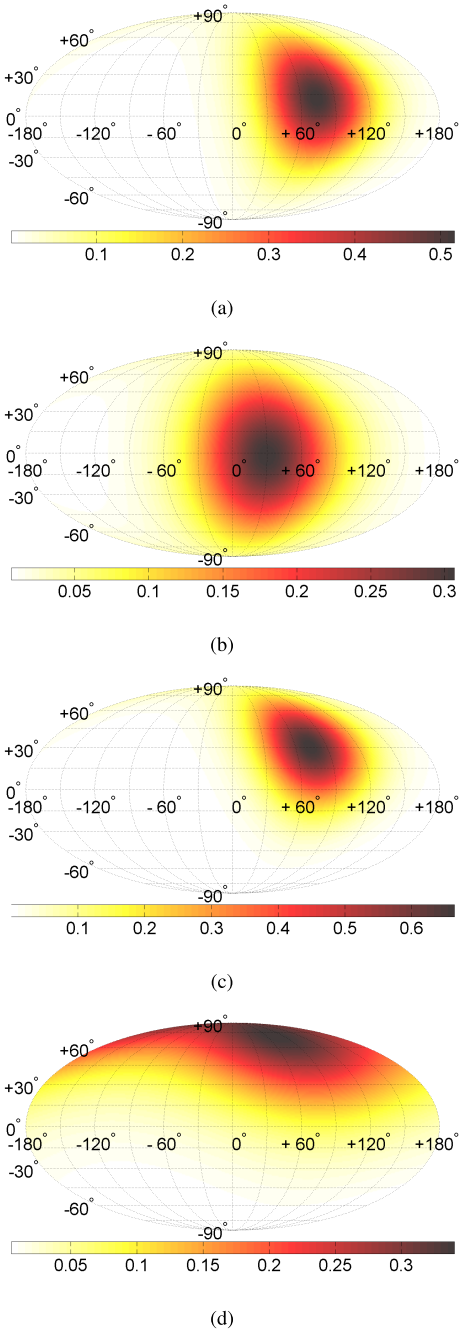

FIGURE 3. 3D von Mises-Fisher probability distribution function represented on a 2D Mollweide map projection for voice users, more specifically for phone usage types; a) 0000, b) 0001, c) 0010 and d) 0100. See Table. 1 and Table. 2 for phone usage type and distribution parameter specification, respectively.

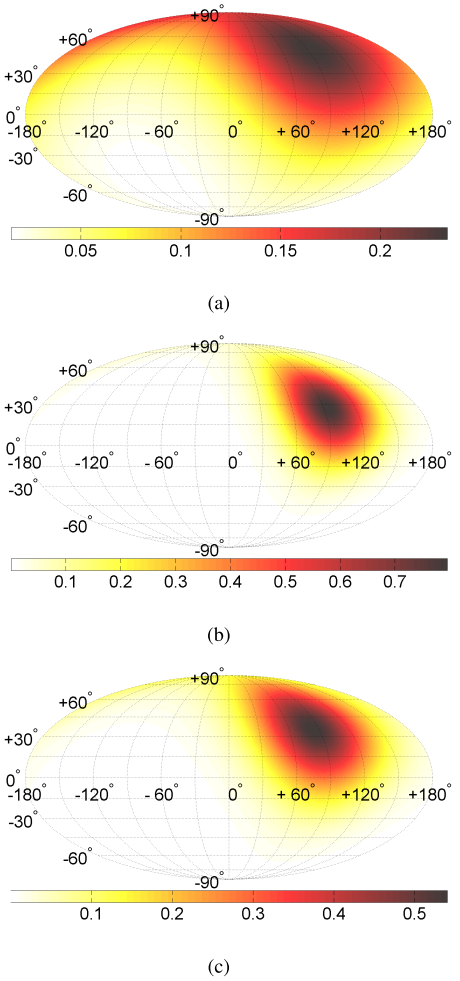

FIGURE 4. 3D von Mises-Fisher probability distribution function represented on a 2D Mollweide map projection for non-voice users, more specifically for phone usage types: a) 1000, b) 1010, and c) 1100. See Table. 1 and Table. 2 for phone usage type and distribution parameter specification, respectively.

4 different brands. Disclosing further details is outside the scope of this paper since we focus on the orientation statistics.

A. DATA PRE-PROCESSING

Prior to proceeding with the model fitting, the accelerometer data was extracted following the binary categories given in Table. 1. Then, outliers were removed following the 1.5*IQR-rule* and duplicate data entries were removed by taking unique values. The same procedure was applied to all phone usage types that could be extracted from the collected data. The phone usage types are listed in the first column in Table. 2.

An example of the results of the data processing is given in Fig. 2. The upper subplot shows the Cumulative Distribution Function (CDF) of the magnitude of the acceleration $\|\boldsymbol{a}\|$ corresponding to the voice service for users that used no wired-headset, no speaker-phone and no Bluetooth-headset. Results are presented for the raw data as downloaded from the app and data that has been processed as explained above. As expected, the applied outlier elimination rule and selecting unique values moved the distribution of $\|\boldsymbol{a}\|$ toward the median, i.e., the gravity acceleration g.

The three lower subplots in Fig. 2 show the Probability Distribution Function (PDF), or rather, the normalized histogram of ρ_{ix}, ρ_{iy}, ρ_{iz} components of the corresponding normalized acceleration vector, i.e., the phone orientation vector (1). As can be seen the data processing efficiently

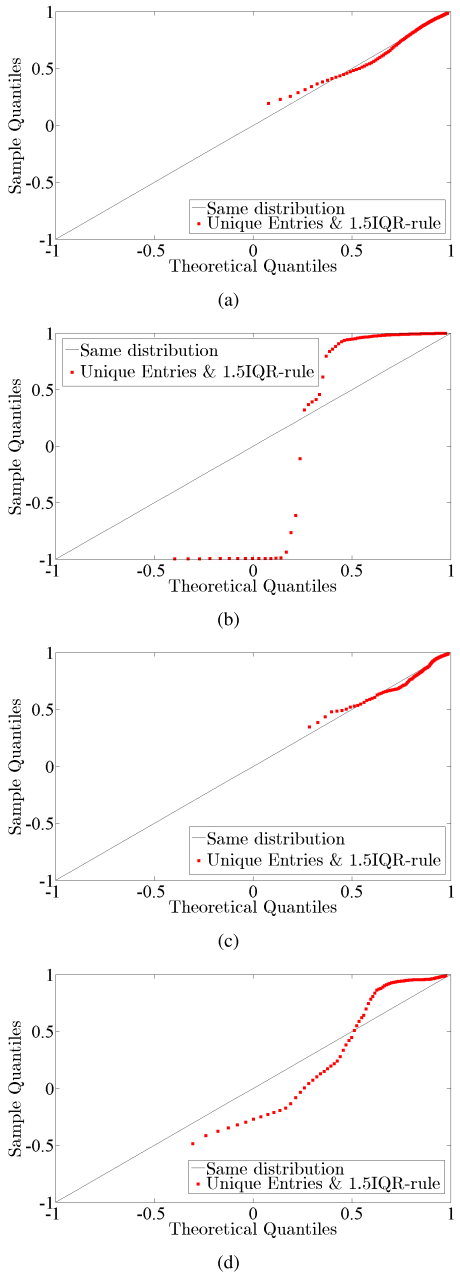

FIGURE 5. Q-Q plots for voice users, more specifically for phone usage types; a) 0000, b) 0001, c) 0010 and d) 0100. See Table. 1 and Table. 2 for phone usage type and distribution parameter specification, respectively.

removed as turned out to be duplicated values in the vicinity of $\rho_{ix} = \rho_{iy} = 0$ and for $\rho_{iz} = 1$. It is worthwhile to recall that corresponding acceleration values where removed prior normalization. Hence, we expect the processed data be more representative of the user-induced randomness due to device orientation. The presented approach should be considered as a straightforward, yet approximate, identification procedure of useful random data samples.

B. VON MISES-FISHER DISTRIBUTION FITTING

Fig. 3 and Fig. 4 show the 3D vMF directional PDFs represented on a 2D Mollweide map projection corresponding

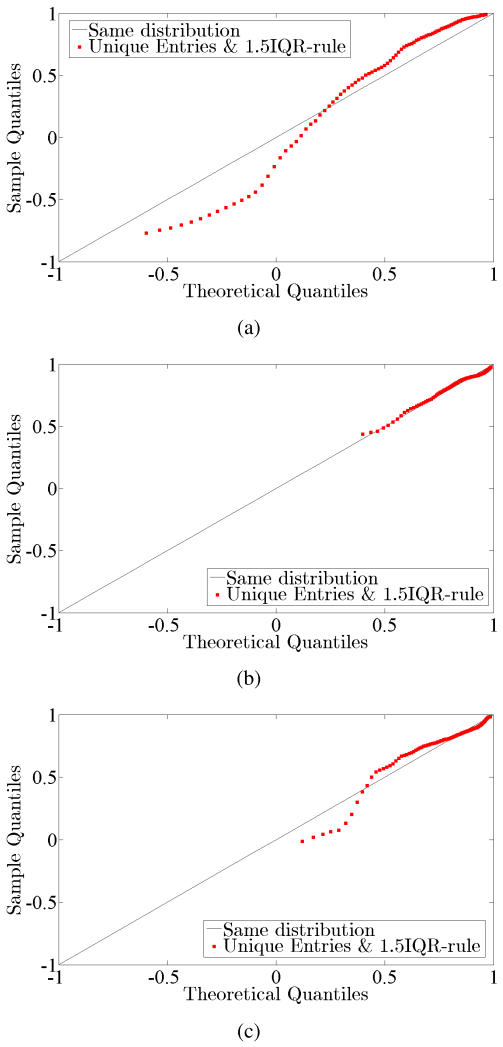

FIGURE 6. Q-Q plots for non-voice users, more specifically for phone usage types; a) 1000, b) 1010, and c) 1100. See Table. 1 and Table. 2 for phone usage type and distribution parameter specification, respectively.

to voice and non-voice phone usage types, respectively. The functions where generated using (3) and using the distribution parameters estimates (see Appendix) given in Table. 2. The presented plots provide a full spherical coverage of the statistical distribution for both voice and non-voice phone usage. We can clearly see the main direction for each usage type, i.e., the mean phone orientation in the different usage orientations. As explained above, the lower the κ parameters the less concentrated values of the orientations around the mean orientation and viceversa.

Fig. 5 and Fig. 6 show the Q-Q plots corresponding to sample vMF distributions v.s. theoretical (simulated) vMF distributions computed with estimated parameters given in Table. 2. Each plot in Fig. 5 and Fig. 6 should be considered in juxtaposition with corresponding plots in Fig. 3 and Fig. 4, respectively. The estimated projection quantiles $\hat{c}_\tau$ where obtained for quantiles $\tau = \{0.05, ..., 0.95\}$ taken in 0.01 steps. Hence, the leftmost point corresponds to $\tau =$

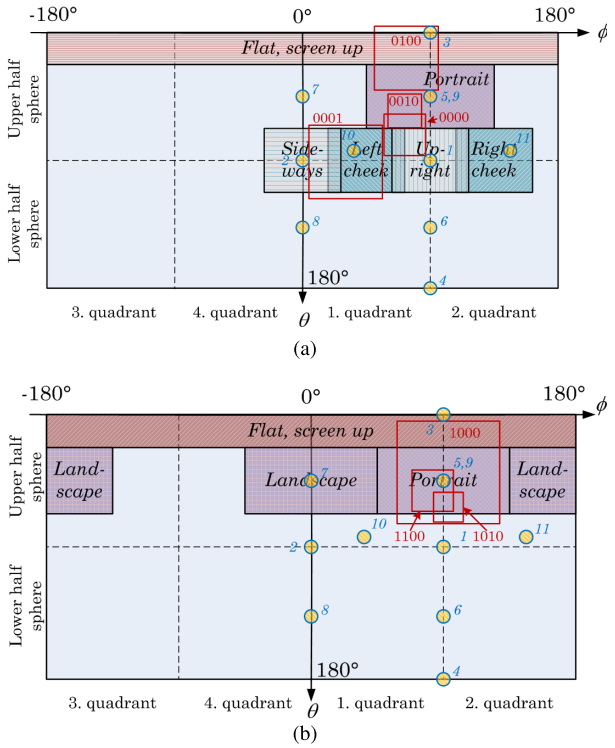

FIGURE 7. ϕ-θ plots showing the location and spreading of the different usage types. Size of squares are inversely proportional to the concentration factor κ; a) voice b) non-voice. See Table. 1 and Table. 2 for phone usage type and distribution parameter specification, respectively. The circles show the OTA test positions as defined by the 3GPP and explained in Table. 3.

0.05 (5%-quantile), while the rightmost point corresponds to $\tau = 0.95$ (95%-quantile). By visual inspection we immediately realize that the proposed vMF model only approximately describes the directional distribution of the data. The best fits correspond to phone usage type 0000, 0010 and 1010, followed by less so models corresponding to phone usage type 1000, 1100 and 0100 and the worst fitting is for phone usage type 0001.

The main reason that may lead to discrepancies between the model and the data samples is the fact that the underlying true empirical distribution is not well-described by a single cluster. Therefore, future models should take into account multiple clusters and a possible correlation between them. However, the presented results may be considered as a first-order approximation describing the user-induced mobile phone orientation randomness. And as shown above, for some specific cases, the vMF is indeed an excellent fit to the statistical distribution of the orientation of the mobile phone.

C. FINITE MIXTURE MODEL FOR USER INDUCED RANDOMNESS

The vMF distribution is indeed a straightforward model that together with parameters provided in Table. 2 gives an easy way to simulate different phone orientations following the algorithm in [18]; also the MATLAB scripts available in [19] can be used. However, we need more, we need a model with as much flexibility as needed to accurately describe the real life data.

The concept of a finite mixture model (FMM) provides us with the desired model flexibility [22]. We may define an FMM of vMF distributions describing different phone usage type as the device orientation vector $\boldsymbol{\rho}$ with the PDF

$$f_{\text{mix}}(\boldsymbol{\rho}; \boldsymbol{\gamma}) = \frac{\sum_{i=0}^{1}\sum_{j=0}^{1}\sum_{k=0}^{1}\sum_{l=0}^{1} \pi_{ijkl} f(\boldsymbol{\rho}; \boldsymbol{\mu}_{ijkl}, \kappa_{ijkl})}{\sum_{i=0}^{1}\sum_{j=0}^{1}\sum_{k=0}^{1}\sum_{l=0}^{1} \pi_{ijkl}}, \tag{4}$$

where $f(\boldsymbol{\rho}; \boldsymbol{\mu}_{ijkl}, \kappa_{ijkl})$ is the vMF distribution with mean direction $\boldsymbol{\mu}_{ijkl}$ and concentration parameters κ_{ijkl} and the weights $\pi_{ijkl} \geq 0$ satisfy the probability normalization

$$\sum_{i=0}^{1}\sum_{j=0}^{1}\sum_{k=0}^{1}\sum_{l=0}^{1} \pi_{ijkl} = 1. \tag{5}$$

The parameter

$$\boldsymbol{\gamma} = \{\boldsymbol{\mu}_{ijkl}, \kappa_{ijkl}, \pi_{ijkl}\} \text{ with } i, j, k, l = \{0, 1\}, \tag{6}$$

denotes the parameter matrix of the FMM. The number of components is itself a parameter of the model.

The drawback is that estimating the parameters of the vMF FMM is not a trivial task and requires a rather sophisticated approach to solving the task at hand [22]. Here, we propose a heuristic approach exploiting the knowledge about the data that we already have. Indeed, since we define the phone usage types, we can then in turn compute the frequency of observing data that correspond to a certain phone usage type π_{ijkl} as

$$\pi_{ijkl} = \frac{N_{\text{s},ijkl}}{\sum_{i=0}^{1}\sum_{j=0}^{1}\sum_{k=0}^{1}\sum_{l=0}^{1} N_{\text{s},ijkl}}, \tag{7}$$

where $N_{\text{s},ijkl}$ denotes the number of samples used to estimate the vMF distribution parameters. Clearly, (7) satisfies the normalization (5). Assuming a vMF FMM that includes all the practical phone usage types, we can then obtain the heuristic weights as given in Table. 2. Terms with missing values are just replaced by 0 in the summations in (4), (5) and (7). In this way we have now computed all the values of the FMM parameter matrix $\boldsymbol{\gamma}$ in (6). The PDF of the vMF FMM is now fully defined, which can be straightforwardly simulated following standard algorithms, e.g., the composition method algorithm [23].

In addition to the above model, other mixture models can be generated with the same procedure when applied to subsets of phone usage types according to Table. 2. For example, it may be interesting to consider usage types when no headsets nor speaker phone are used. In that case the vMF FMM distribution is computed by with the help of the parameters corresponding to phone usage types 0000 and 1000 in Table. 2. It is worthwhile to note that in this case the weights π_{0000} and π_{1000} do not sum up to 1. However, the formulation of the vMF FMM (4) guaranties that the

TABLE 3. OTA test conditions as defined by the 3GPP [21].

Index	3GPP test condition	Comment
1	XY-plane	Vertical upright
2	XZ-plane	Vertical sideways
3	Free space data mode (FS-DMSU)	Horizontal, screen up
4	Face down	Horizontal. screen down
5	Free space data mode portrait (FS-DMP)	Portrait, tilted
6	Free space tilted down	Portrait, downtilted
7	Free space data mode landscape (FS-DML)	Landscape, tilted
8	Free space landscape, tilted down	Landscape, downtilted
9	Left/right hand phantom data mode portrait (LH/RH-DMP)	Portrait, tilted
10,11	Beside head and hand right/left (BHHR/BHHL)	Cheek right and cheek left

TABLE 4. Matching phone usage types and CTIA/3GPP test conditions.

Ph. Usage $\{ijkl\}$	3GPP Test Cond.	Comment
0000	1	Voice, no wired or wireless headset. Vertical upright
0001	10	Voice, Bluetooth on. Vertical slant
0010	5,9	Voice, speakerphone. Portrait, tilted
0100	3	Voice, wired headset. Horizontal screen up
1000	5,9	Non-voice, no wired or wireless headset. Portrait, tilted
1010	1,5,9	Non-voice, speakerphone. Portrait, vertical to tilted
1100	5,9	Non-voice, wired headset. Portrait, tilted

renormalized weights $\frac{\pi_{0000}}{\pi_{0000}+\pi_{1000}}$ and $\frac{\pi_{1000}}{\pi_{0000}+\pi_{1000}}$ do sum up to 1 as required.

Hence, differentiating the most common phone usages for the two main services enables a systematic modelling of the device orientation, with applications to OTA testing, to wireless network analysis and optimization, to radio wave propagation and indoor localization.

D. MAPPING PHONE USAGE TYPES TO TYPICAL USAGE POSITIONS

In [11], the concept of *user modes* was introduced. The hypothesis is that certain ways of holding the phone should dominate depending on the services accessed. For voice usage it is expected that use of handsfree, whether wired, Bluetooth or loud-speaker, would be different than without. We see from the vMF distribution parameters in Table 2 that this is the case. Traditional usage for voice calls would be holding the phone to either right or left cheek, while handsfree usage could include a number of modes. For non-voice usage, we could expect that some kind of slant holding positions, either portrait or landscape mode would be typical, but also having the phone lying horizontally on a flat surface.

Industry and standards organizations CTIA and 3GPP has developed test plans for OTA performance measurements of user equipment [21], [24]. Here, fixed orientation conditions for Equipment Under Test (EUT) has been defined, including a number of EUT orientation angles. These correspond to our definition of user modes, and some anticipated modes are drawn in the ϕ-θ coordinate system in Fig. 7 together with the found statistics from Table 2. The user modes corresponding to the CTIA and 3GPP orientation angles are shown in the same figures and explained in 3. For voice usage, we see that an upright position tending towards left cheek is common without handsfree (usage type 0000), while handsfree usage results in more slant positions. Use of wired handsfree is near to horizontal flat mode. For non-voice usage, most usage types maps to portrait orientation, except the use of speaker which shows a vertical position.

The statistics analysis in [11] showed that there are multiple clusters, especially for usage type 0000, and that is missed here, as discussed in subsection IV-B. Two quite visible peaks on left cheek and right cheek was visible, where the left position was most common. The preference for left cheek is only visible by the centre position of the 0000 usage type.

The CTIA and 3GPP defined orientation angles are not given as distributions, but as fixed points. As can be seen from Tables 3 and IV-C, only some of the definitions seem relevant. For example, for voice usage this are 3, 5/9 and 10, while for non-voice usage it is basically 5/9. Orientations corresponding to test conditions 2, 4, $6-8$ and 11 are not observed. It is worthwhile to note that the model is not handling distributions with multiple maxima.

V. CONCLUSIONS AND FUTURE WORK

In this paper we have shown how smart-phone sensors can be used to model a wireless device usage in real-life situations without the intervention of the experimenter. This information can have a profound repercussion on the design

of better handsets, but also to improve wireless network performance.

Indeed, the proposed von Mises-Fisher directional distribution provides a statistical model for the phone's orientation over the full sphere for different *phone usage types*, e.g., voice or non-voice services used in combination with wired or Bluetooth handsfree connection or a speaker. Also different mixes of phone usage types can be studied and simulated based on their individual distributions by the finite mixture model approach. The heuristic weights of the mixture model are computed as the frequency of observation of data samples belonging to the different phone usage types. Hence, statistical distributions describing phone usage types in voice and non-voice modes can be generated and incorporated, e.g., in Random-LOS OTA performance analysis, channel model generation and wireless network design and optimization.

The model is based on analysing the acceleration (gravity) vector data obtained from accelerometer sensor readings in real life. However, the analysis of the data collected from the users may not be fully representative of the actual user-induced mobile phone orientation randomness since data is limited to 11 users so far. However, the number of users reporting their accelerometer data will increase in the future, e.g., by means of crowdsourcing. This will provide a more representative data set of the phone usage types and therefore improve the randomness characterization of the users.

In addition, future work could also take into account more diverse factors such as usage differentiation over time, e.g., day or night, and among the users' age, e.g., youth, middle age or elderly. This type of data, if made available, could be useful to develop targeted applications. Also, in future analysis more sophisticated data pre-processing (i.e., before the statistical parameters are estimated) will be needed in order to fine-tune the statistical models of the different phone usage types. For example, the finite mixture model could be applied to each usage type separately to identify clustering effects that might have been gone unnoticed by removing duplicate data, i.e., the pre-processing approach we have used in our analysis. Another interesting research direction is developing more sophisticated goodness of fit test for spherical statistical models.

APPENDIX

Let $\chi_{\boldsymbol{\rho}} = \{\boldsymbol{\rho}_1, \ldots, \boldsymbol{\rho}_N\}$ be a set of points drawn from $f(\boldsymbol{\rho}; \boldsymbol{\mu}, \kappa)$ (3). The estimates $\hat{\boldsymbol{\mu}}$ and $\hat{\kappa}$ that maximize the log-likelihood function

$$\mathcal{L}(\chi_{\boldsymbol{\rho}}; \boldsymbol{\mu}, \kappa) = N \ln\left(\frac{\kappa}{4\pi \sinh(\kappa)}\right) + \sum_{i=1}^{N} \kappa \boldsymbol{\mu}^{\mathrm{T}} \boldsymbol{\rho}_i, \quad (8)$$

subject to the condition that $\boldsymbol{\mu}^{\mathrm{T}}\boldsymbol{\mu} = 1$ and $\kappa \geq 0$ are given by [17]

$$\hat{\boldsymbol{\mu}} = \frac{\sum_{i=1}^{N} \boldsymbol{\rho}_i}{\| \sum_{i=1}^{N} \boldsymbol{\rho}_i \|}, \quad (9)$$

$$\hat{\kappa} = A_3^{-1}(\bar{R}), \quad (10)$$

where

$$\bar{R} = N^{-1} \| \sum_{i=1}^{N} \boldsymbol{\rho}_i \|, \quad (11)$$

$$A_3(\kappa) = I_{3/2}(\kappa)/I_{1/2}(\kappa), \quad (12)$$

where I_ν denotes the modified Bessel function of the first kind of order ν [25]. Hence, $\hat{\kappa}$ is the solution to $A_3(\kappa) - \bar{R} = 0$, that is obtained numerically by the Newton's method

$$\kappa_0 = \frac{\bar{R}(3 - \bar{R}^2)}{1 - \bar{R}}, \quad (13)$$

$$\kappa_k = \kappa_{k-1} - \frac{A_3(\kappa_{k-1}) - \bar{R}}{1 - A_3(\kappa_{k-1})^2 - \frac{2}{\kappa_{k-1}} A_3(\kappa_{k-1})}, \quad (14)$$

where κ_0 is the initial value and the iteration usually converges after two steps, and thus $\hat{\kappa} = \kappa_2$.

ACKNOWLEDGMENT

Great part of this work was inspired by the late Prof. Per-Simon Kildal.

REFERENCES

[1] A. A. Glazunov, V.-M. Kolmonen, and T. Laitinen, "MIMO over-the-air testing," in *LTE-Advanced and Next Generation Wireless Networks: Channel Modelling and Propagation*, G. de la Roche, A. A. Glazunov, and B. Allen, Eds. Hoboken, NJ, USA: Wiley, 2012, pp. 411–442.

[2] P. S. Kildal and K. Rosengren, "Correlation and capacity of MIMO systems and mutual coupling, radiation efficiency, and diversity gain of their antennas: Simulations and measurements in a reverberation chamber," *IEEE Commun. Mag.*, vol. 42, no. 12, pp. 104–112, Dec. 2004.

[3] P. S. Kildal, C. Orlenius, and J. Carlsson, "OTA testing in multipath of antennas and wireless devices with MIMO and OFDM," *Proc. IEEE*, vol. 100, no. 7, pp. 2145–2157, Jul. 2012.

[4] A. Razavi, A. A. Glazunov, P. S. Kildal, and J. Yang, "Characterizing polarization-MIMO antennas in random-LOS propagation channels," *IEEE Access*, vol. 4, pp. 10067–10075, 2016.

[5] A. Razavi and A. A. Glazunov, "Probability of detection functions of polarization-MIMO systems in random-LOS," *IEEE Access*, vol. 5, pp. 25635–25645, 2017.

[6] E. Mellios, Z. Mansor, G. S. Hilton, A. R. Nix, and J. P. McGeehan, "Impact of antenna pattern and handset rotation on macro-cell and pico-cell propagation in heterogeneous LTE networks," in *Proc. IEEE Antennas Propag. Soc. Int. Symp. (APSURSI)*, Jul. 2012, pp. 1–2.

[7] P.-S. Kildal, "Rethinking the wireless channel for OTA testing and network optimization by including user statistics: RIMP, pure-LOS, throughput and detection probability," in *Proc. Int. Symp. Antennas Propag. (ISAP)*, vol. 1, Oct. 2013, pp. 1–9.

[8] P.-S. Kildal and J. Carlsson, "New approach to OTA testing: RIMP and pure-LOS reference environments & a hypothesis," in *Proc. 7th Eur. Conf. Antennas Propag. (EuCAP)*, Apr. 2013, pp. 315–318.

[9] P.-S. Kildal, A. A. Glazunov, J. Carlsson, and A. Majidzadeh, "Cost-effective measurement setups for testing wireless communication to vehicles in reverberation chambers and anechoic chambers," in *Proc. IEEE Conf. Antennas Meas. Appl. (CAMA)*, Nov. 2014, pp. 1–4.

[10] P. H. Lehne, K. Mahmood, A. A. Glazunov, P. Grønsund, and P.-S. Kildal, "Measuring user-induced randomness to evaluate smart phone performance in real environments," in *Proc. 9th Eur. Conf. Antennas Propag. (EuCAP)*, Apr. 2015, pp. 1–5.

[11] P. H. Lehne, A. A. Glazunov, K. Mahmood, and P.-S. Kildal, "Analyzing smart phones' 3D accelerometer measurements to identify typical usage positions in voice mode," in *Proc. 10th Eur. Conf. Antennas Propag. (EuCAP)*, Apr. 2016, pp. 1–5.

[12] K. V. Mardia and P. E. Jupp, *Directional Statistics*, vol. 494. Hoboken, NJ, USA: Wiley, 2009.

[13] *Android Sensor Event*. Accessed: Oct. 13, 2015. [Online]. Available: http://developer.android.com/reference/android/hardware/SensorEvent.html

[14] D. Mizell, "Using gravity to estimate accelerometer orientation," in *Proc. 7th IEEE Int. Symp. Wearable Comput.*, Oct. 2003, pp. 252–253.
[15] J. R. Blum, D. G. Greencorn, and J. R. Cooperstock, "Smartphone sensor reliability for augmented reality applications," in *Mobile and Ubiquitous Systems: Computing, Networking, and Services* (Lecture Notes of the Institute for Computer Sciences, Social Informatics and Telecommunications Engineering), vol. 120, K. Zheng, M. Li, and H. Jiang, Eds. Berlin, Germany: Springer, 2013, pp. 127–138, doi: 10.1007/978-3-642-40238-8_11.
[16] Z. Ma, Y. Qiao, B. Lee, and E. Fallon, "Experimental evaluation of mobile phone sensors," in *Proc. 24th IET Irish Signals Syst. Conf. (ISSC)*, Jun. 2013, pp. 1–8.
[17] S. Sra, "A short note on parameter approximation for von Mises-Fisher distributions: And a fast implementation of $I_s(x)$," *Comput. Statist.*, vol. 27, no. 1, pp. 177–190, 2012.
[18] A. T. A. Wood, "Simulation of the von Mises Fisher distribution," *Commun. Statist.-Simul. Comput.*, vol. 23, no. 1, pp. 157–164, 1994. [Online]. Available: http://dx.doi.org/10.1080/03610919408813161
[19] Y.-H. Chen. *Spherical Distribution Random Variable Generation*. Accessed: Jun. 2017. [Online]. Available: http://www.mathworks.com/matlabcentral/fileexchange/52398-sphericaldistributionsrand
[20] C. Ley, C. Sabbah, and T. Verdebout, "A new concept of quantiles for directional data and the angular Mahalanobis depth," *Electron. J. Statist.*, vol. 8, no. 1, pp. 795–816, 2014. [Online]. Available: http://dx.doi.org/10.1214/14-EJS904
[21] *Technical Specification Group Radio Access Network; Universal Terrestrial Radio Access (UTRA) and Evolved Universal Terrestrial Radio Access (E-UTRA); Verification of radiated multi-antenna reception performance of User Equipment (UE) (Release 14)*, 3GPP Standard TR 37.977 V14.2.0, 3GPP, Dec. 2016.
[22] G. McLachlan and D. Peel, *Finite Mixture Models*. Hoboken, NJ, USA: Wiley, 2004.
[23] D. P. Kroese, T. Taimre, and Z. I. Botev, *Handbook of Monte Carlo Methods*, vol. 706. Hoboken, NJ, USA: Wiley, 2013.
[24] *Test Plan for 2×2 Downlink MIMO and Transmit Diversity Over-the-Air Performance Version 1.1*, CTIA, Washington, DC, USA, Aug. 2016.
[25] I. S. Gradshteyn and I. M. Ryzhik, *Table of Integrals, Series, and Products*, 6th ed. New York, NY, USA: Associated Press, 2000.

ANDRÉS ALAYÓN GLAZUNOV (SM'11) was born in Havana, Cuba, in 1969. He received the M.Sc. (Engineer-Researcher) degree in physical engineering from Peter the Great St. Petersburg Polytechnic University, Russia, in 1994, the Ph.D. degree in electrical engineering from Lund University, Sweden, in 2009, and the Docent (Habilitation) degree in antenna systems from the Chalmers University of Technology, Gothenburg, Sweden, in 2017. From 1996 to 2005, he held various research and specialist positions in the Telecom industry, e.g., Ericsson Research, Kista, Sweden, and Telia Research and TeliaSonera, Farsta, Sweden. From 2001 to 2005, he was the Swedish delegate to the European Cost Action 273 and was active in the Handset Antenna Work Group. He has been one of the pioneers in establishing OTA measurement techniques. He has contributed to and initiated various European research projects, e.g., currently, the is3DMIMO, the WAVECOMBE, and the Build-Wise projects under the auspices of the H2020 European Research and Innovation program. He has also contributed to the international 3GPP and the ITU standardization bodies. From 2009 to 2010, he was a Marie Curie Senior Research Fellow with the Centre for Wireless Network Design, University of Bedfordshire, U.K. From 2010 to 2014, he held a post-doctoral position with the Electromagnetic Engineering Laboratory, KTH-Royal Institute of Technology, Stockholm, Sweden. From 2014 to 2018, he was an Assistant Professor with the Chalmers University of Technology.

He is currently an Associate Professor with the Department of Electrical Engineering, University of Twente, Enschede, The Netherlands, where he is leading the radio, propagation and antenna systems research lab. He is also with the Chalmers University of Technology, Gothenburg, Sweden, where he is leading the OTA characterization of antenna systems research area. He has authored over 100 scientific and technical publications. He has co-authored and co-edited the text book *LTE-Advanced and Next Generation Wireless Networks: Channel Modelling and Propagation* (Wiley, 2012). His current research interests include, but are not limited to MIMO antenna systems, electromagnetic theory, fundamental limitations on antenna-channel interactions, radio propagation channel measurements, modeling and simulations, and the OTA characterization of antenna systems and wireless devices.

PER HJALMAR LEHNE received the M.Sc. degree from the Norwegian Institute of Science and Technology in 1988. He has been with Telenor Research since 1988 involved in different aspects of terrestrial mobile communications, where he is currently a Senior Researcher. Since 1993, he has been involved in radio propagation and access technology, especially on multiple antenna systems and radio access technologies (GSM, UMTS, and LTE). He has also been involved in spectrum management techniques and cognitive radio research. He has previously participated in several international research projects in the EU framework, as well as COST actions in the field. He is currently a Management Committee Member of COST CA15104 IRACON.